



CDF/PUB/MIN_BIAS/PUBLIC/9936

Multiplicity Distribution of Charged Particles in Inelastic $p\bar{p}$ Interactions

The CDF Collaboration

URL <http://www-cdf.fnal.gov>

(Dated: September 22, 2009)

The multiplicity distribution of charged particles is measured in inelastic non-diffractive $p\bar{p}$ collisions at $\sqrt{s} = 1.96$ TeV. The data were collected using the Collider Detector at Fermilab (CDF) experiment during RunII of the Fermilab Tevatron collider. This analysis is part of a systematic and detailed set of measurements of minimum-biased events. The data presented here have the highest precision and the largest range extension ever reached in the pseudorapidity range $|\eta| \leq 1$.

I INTRODUCTION

In a recent paper [1] we reported the measurement of the inclusive charged particle transverse momentum differential cross-section in the Minimum-Bias sample. Here we extend those studies with the measurement of the charged particle multiplicity distribution.

The multiplicity distribution in inelastic hadron interactions has always been a complicated puzzle. A number of models have been proposed to describe this distribution [2][3]. None of them has successfully survived to more precise measures and/or to the advent of data from higher c.m. energies. Most models could readily be tuned to give an acceptable description of many single minimum-bias observables, but none could describe simultaneously the entire set. The multiplicity distribution represent an important test since many perturbative and non-perturbative effects contribute to it; also effects due to multiple parton-parton interactions must be accounted for.

The data presented here have the highest precision and the largest range extension ever reached in the phase space region $|\eta| < 1$ and $p_T > 0.4$ GeV/ c . This makes of the new measurement an important handle for the understanding the interplay of the particle production mechanisms involved and for the tuning of Monte Carlo (MC) models. It will allow more reliable extrapolations to LHC energies [4] and more precise estimates of soft QCD background in high- p_T measurements. This study is part of a systematic set of measurements part of which have been published in [1].

Full corrections of effects due to trigger acceptance, particle detection inefficiencies and background contamination from diffractive events are applied. A comparison with the PYTHIA Monte Carlo generator model (v6.2) is also carried out.

The CDF detector is described in detail in [5].

II DATA SAMPLES

The analysis is based on a data sample collected between October 2002 and August 2004 with an integrated luminosity of 506 pb⁻¹. The average instantaneous multiplicity of the sample is 20E30 cm⁻²s⁻¹. The data were collected with a Minimum-Bias (MB) trigger that requires a coincidence in time of signals from the Tevatron radiofrequency and in both forward and backward CLC modules [6].

The MB trigger is designed to collect, with uniform acceptance, events from all possible inelastic interactions. At the energy of the Tevatron, MB data consist largely of the softer interactions. In this study, only the inelastic particle production in the central part of the region orthogonal to the beam axis is exploited. The diffractive interactions are neglected.

To increase the statistics in the high-multiplicity region where the cross sections vanishes, this analysis also uses data collected with a dedicated “high-multiplicity” trigger that selects events that passed the MB trigger precondition and in addition have a large number of primary charged particles. This trigger collected about 64,000 events in the same data-taking period of the MB sample.

An offline event selection is applied to the recorded samples. Events that contain cosmic-ray candidates, identified by the combination of tracking and calorimeter timing, are rejected. Only those events collected when all the detector components were working correctly are included in the final reduced data sample.

Because of their dependence on the number of tracks in the bunch crossing, a variable closely related to the event particle multiplicity, both the trigger and the vertex efficiencies affect not only the total cross section but also the shape of inclusive distributions. The efficiency values are computed on an event-by-event basis.

A Trigger and Vertex Acceptance

Due to small inefficiencies in the response of the CLC detector, the minimum-bias trigger is not fully efficient. Its efficiency has been evaluated by monitoring the trigger with several central high transverse energy triggers. The results show that the trigger efficiency increases with the increase of some global event variables such as central multiplicity and central sum E_T .

On the other hand, the total acceptance (including the efficiency) of the trigger has been measured by comparing it with a sample of zero-bias events collected during the same period. The zero-bias data set is collected without any trigger requirements, simply by starting the data acquisition at the Tevatron radio-frequency signal. The results are in agreement with previous studies [7] and indicate that the efficiency depends on a number of variables, most of which in some way are related to the number of tracks present in the detector, and on the CLC calibration. We parametrized the dependence on these variables and obtain a

correction factor which can be applied on an event-by-event basis.

The total MB trigger acceptance increases linearly with the instantaneous luminosity. As a function of the number of tracks, the acceptance is well represented by a typical turn-on curve starting at about 20% (two tracks) and reaching its plateau) with a value between 97 and 99% for about 15 tracks.

The “high-multiplicity” trigger functions at Level 1 by selecting events with at least 14 hit bars in the TOF system [8], a hit being defined as the coincidence of two signals from the photomultipliers at the two ends of each bar. At Level 3 it requires at least 22 reconstructed tracks converging to the event vertex. This setting ensures that no other bias – except for the high number of tracks – is imposed to the data collected. The efficiency is higher than 97%.

The primary vertex recognition efficiency for the MB data sample is evaluated in two ways: by comparing the number of expected vertices on the basis of the instantaneous luminosity and by using a Monte Carlo simulation with multiple $p\bar{p}$ interactions. This efficiency was studied as a function of various event variables and found to be roughly flat for $|z| \leq 40$ cm, but strongly dependent on the number of interactions in the bunch crossing and on the number of tracks available for vertex clustering. Therefore the efficiency has been parametrized as a function of the number of tracks and of the instantaneous luminosity.

B Event Selection

This analysis rejects interactions that contain more than one primary vertex in the fiducial region $|z_{vtx}| \leq 40$ cm centered around the nominal CDF $z = 0$ position. A total of 9,788,632 events were selected.

Primary vertices are identified by the convergence of reconstructed tracks along the z -axis. The event selection described contains an unavoidable contamination due to multiple vertices when the separation between vertices is less than the vertex resolution in the z -coordinate, which is about 3 cm. A correction for this effect is discussed in Sec. VI.

C Merging of the High-Multiplicity Trigger Sample

In the region of multiplicity ≥ 23 the minimum-bias and the high-multiplicity raw data sample distributions have been merged by computing the weighted average bin-by-bin. The weights are taken to be the square of the inverse of the statistical relative uncertainties.

In order to check that the two samples actually yield the same cross sections, we compare the raw distributions taken from (a) the full high-multiplicity sample and (b) a subsample of MB corresponding to the same runs as the previous sample. Each distribution is scaled by the effective luminosity of the corresponding sample so to represent a “trigger cross section”. In the range of multiplicity ≥ 23 the normalization of the two distributions differs only of 1.1%.

All the corrections discussed in the following sections are applied to the distribution obtained by merging the two samples.

D Backgrounds

Diffractive events, with final-state particles mostly confined in the forward regions, may have some activity in the central region that enters as a background in our sample. By assuming the following indicative values $\sigma_{ci}/\sigma_{sd}/\sigma_{dd} = 44.4/10.3/7.0$ mb for the central-inelastic, single-, and double-diffractive cross sections [9], respectively, and knowing the relative CLC acceptances, we estimate their contribution to the MB cross section to be approximately 6%. Roughly the same conclusion was drawn by analyzing a sample of diffractive events generated with the PYTHIA simulation and passed through a MB trigger simulation. Considering that in about half of the diffractive events no primary vertex is reconstructed, we estimate that diffractive production forms up to 3.4% of our MB sample and is concentrated in the region of low charged particle multiplicity.

E Event Pile-Up

Even in the low luminosity condition of our dataset, after selecting interactions with only one primary vertex some undetected “pile-up” of events may affect the multiplicity distribution. This pile-up is generated by events that are produced closer than about 3 cm

along the z -axis. In this case the resolution of the primary vertex position is too poor to distinguish the two interactions so that their tracks are merged into a single interaction.

This effect can be clearly seen by plotting the average event multiplicity as a function of the luminosity, fig.1: the multiplicity increases with the instantaneous luminosity.

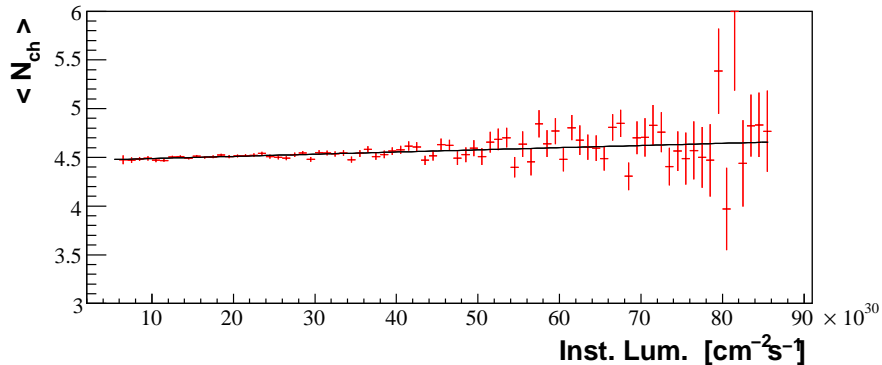


FIG. 1: Average raw multiplicity as a function of the instantaneous luminosity.

A first estimate of such pile-up may be easily extracted from the generator-level simulation. In our MC Pythia sample, the number of events generated within ± 3 cm from another event is 2.9%. Since our MC does not reproduce the instantaneous luminosity shape of the run, but only the average run luminosity, this value is probably overestimated.

Therefore the amount of the undetected pile-up was estimated by theoretical calculation. The average number of interactions per crossing may be obtained from the inelastic cross section [10] once the average luminosity and the rate of crossings are known. The probability of multiple interactions is given by a Poisson distribution of mean $\langle n \rangle$. After selecting interactions with at least one event $\langle n \rangle \simeq 0.31$. We estimate from MC that for events with $|z| < 40$ cm the fraction of pile-up within ± 3 cm is 8% of all pile-up crossing. With this, the probability of undetected pile-up is approximately $0.31 \times 0.08 = 0.025$. This value includes both pile-up of central-inelastic and of diffractive events.

In conclusion, we take 2.5%, to be the correct fraction of events that contain an undetected pile-up.

F The Monte Carlo Sample

A sample of simulated Monte Carlo events about twice the size of the data was generated with PYTHIA version 6.216 [11], with parameters optimized for the best reproduction of minimum-bias interactions. PYTHIA Tune A [12] describes the MB interactions starting from a leading order QCD $2 \rightarrow 2$ matrix element augmented by initial- and final-state showers and multiple parton interactions [13], folded in with CTEQ5L parton distribution functions [14] and the Lund string fragmentation model [15]. To model the mixture of hard and soft interactions, PYTHIA introduces a \hat{p}_{T^0} cut off parameter [16] that regulates the divergence of the 2-to-2 parton-parton perturbative cross section at low momenta. This parameter also regulates the additional parton-parton scatterings that may occur in the same collision. The amount of hard scattering in simulated MB events is, therefore, related to the activity of the so-called underlying event in the hard scattering processes. The final state, likewise, is subject to several effects such as the treatments of the beam remnants and color (re)connection effects.

The MC sample used for all the efficiency and acceptance corrections was generated with Tune A and $\hat{p}_{T^0} = 1.5 \text{ GeV}/c$. This tuning was found to give the same output as the default ($\hat{p}_{T^0} = 0$) with only slightly better reproduction of the high p_T spectrum and a somewhat larger particle multiplicity distribution. A run-dependent simulation with a realistic distribution of multiple interactions was employed. Events were fully simulated through the detector and successively reconstructed with the standard CDF reconstruction chain. The simulation includes the CLC detectors used to trigger the MB sample. The MC sample agrees with data within 10% for inclusive charged particle p_T up to about $20 \text{ GeV}/c$ [1] and η distributions.

The definition of primary particles was to consider all particles with mean lifetime $\tau > 0.3 \times 10^{-10} \text{ s}$ produced promptly in the $p\bar{p}$ interaction, and the decay products of those with shorter mean lifetimes. With this definition strange hadrons are included among the primary particles, and those that are not reconstructed are corrected for. On the other hand, their decay products (mainly π^\pm from K_S^0 decays) are excluded, while those from heavier flavor hadrons are included.

III TRACK SELECTION AND ACCEPTANCE

Reconstructed tracks are accepted if they comply with a minimal set of quality selections including a minimum number of hits, both in axial and stereo layers of the COT. These requirements are made more stringent if no hits in the silicon detectors are used.

All tracks are required to originate in a fiducial region in the plane $(d_0; \Delta z)$, where d_0 is the nearest distance, projected in the transverse plane, between the track extrapolation and the beam axis; Δz is the distance between the point of closest approach of the track to the z -axis and the z -coordinate of the event vertex. The actual region selected in the $(d_0; \Delta z)$ plane depends on the track itself. Tracks reconstructed including the information from silicon detectors are selected within $|d_0| < 0.1$ cm; those reconstructed with no information from the silicon detectors have worse resolution in d_0 , and are accepted if $|d_0| < 0.5$ cm. A similar selection criterion is used along the beam axis: $\Delta z < 1$ cm for tracks with silicon information and $\Delta z < 2$ cm for the remaining tracks. These track selection criteria are used to select primary tracks, and were determined from MC simulation as the ones that maximize the ratio of primary to secondary particles.

As a further requirement, primary charged particles must have a transverse momentum greater than 0.4 GeV/ c and pseudorapidity $|\eta| \leq 1$ in order to optimize the efficiency and acceptance conditions.

The number of primary charged particles in the event after the above selection is defined as the event multiplicity N_{ch} .

A Tracking Efficiency

The tracking efficiency was evaluated in a previous paper [1]. This efficiency may not be used directly to correct the multiplicity distribution, but it is interesting in order to form a general idea of the detector efficiency and of the level of contamination of secondary particles (particle interaction, pair creation), particle decays and mis-identified tracks.

The tracking efficiency is strongly dependent on the number of tracks with a trajectory passing close to the event vertex. As a function of the particle p_T , it is about 70% at $p_T = 0.4$ GeV/ c and increases to about 92% at 5 GeV/ c , where it reaches a plateau. It is roughly flat in η and ϕ , and shows two broad peaks in z that correspond to the edges of the

silicon detector barrels. The fraction of secondary and mis-identified tracks ranges between 1 and 3%.

IV CORRECTION OF THE RAW DISTRIBUTION

A Undetected Pile-Up

In order to correct the effect of undetected pile-up the following method is applied. From MC two multiplicity distributions of events that are overlapping within 3 cm are obtained: one for “central+central” and one for “central+diffractive” events. The first is scaled to $0.025 \times 0.52 = 1.3\%$ of the raw distribution measured from data and the second to $0.025 \times 0.4 = 1\%$. Then both are subtracted bin-by-bin from the raw data distribution. The “diffractive+diffractive” pile-up has negligible effect. The final correction is roughly linear with N_{ch} and ranges from about 1.05 to 0.8.

B Inclusive Method

In order to correct the multiplicity distribution we consider two methods, both based on the same MC simulation and therefore not completely independent. Note that the MC used for computing all the corrections has the CLC simulation active and therefore simulates the MB trigger.

In order to get a first quick estimate of the correction, we divide bin-by-bin the reconstructed (REC) to the particle-level (GEN) Monte Carlo N_{ch} distributions:

$$C_{inc} = \frac{N_{ch}^{REC}(N_{pv} = 1, N_{pp} = 1)}{N_{ch}^{GEN}(N_{pp} = 1)} \quad (1)$$

Since the pile-up is corrected separately, here we take care to select interactions where only one event was originally generated ($N_{pp} = 1$).

The correction can hardly be measured in $N_{ch} \gtrsim 40$ where there are no entries in the reconstructed distribution (while the true distribution still shows some events). The problem may be resolved by adding to our simulation a sample of Pythia dijet events with $\hat{p}_T = 10 \text{ GeV}/c$ (“dijet-10”). For events with $N_{ch} \gtrsim 35$ the two samples have been shown to have similar final states and indeed the inclusive efficiencies are very close in this region.

This correction dumps the probability of events with $N_{ch} \leq 3$ and increases the probability of events with $N_{ch} \geq 10$ of a factor ~ 5 .

A main disadvantage in this kind of correction is that the MC does not reproduce the data multiplicity distribution very well so that the correction is strongly dependent on the MC generator. We use this result only as a cross-check.

C Unfolding Method

This method has the advantage to be less dependent on the MC generator since it allows to reweight the MC generated multiplicity distribution so that it follows the data distribution. The correction procedure is in five steps.

1- Absolute correction $C(N_{ch})$.

The number of reconstructed tracks is modified event-by-event as follows. With MC a scatter plot of the GEN to the REC number of tracks is produced; once more, to gain more statistics in the high-multiplicity region, the dijet-10 MC sample has been added to the minbias sample. For each REC multiplicity the GEN distribution is fit with an asymmetric Gaus function. The distributions are peaked at a N_{ch} GEN value that is 1 to 4 units higher than the REC value. For each event a random number is generated under the fitted function and is taken to be the correct N_{ch} .

2- Extraction of an unfolding factor.

The distribution must now be "unfolded" to smear the resolution effects of the $C(N_{ch})$ correction. An unfolding factor is computed bin-by-bin with MC as

$$U = \frac{N_{ch}^{GEN}(N_{pv} = 1, N_{pp} = 1)}{N_{ch}^{REC}(N_{pv} = 1) \times PU/C(N_{ch})}$$

where PU is the correction for pile-up and $C(N_{ch})$ the absolute correction of N_{ch} described above. The absolute correction $C(N_{ch})$ is applied event-by-event on MC as well as on data. A cross-check is done to ensure that the unfolding applied to the reconstructed MC distributions returns equal to the generated MC distribution.

3- Extraction of the weights to reweight the MC distribution.

The unfolding U is applied to the data raw distribution to obtain a first corrected distribution. With this, a set of weights is computed that are used to re-weight the

MC generated distribution so that it follows the corrected data. Weights are computed, for each multiplicity, as

$$W = \frac{N_{ch}^{data}(N_{pv} = 1) \times PU/C(N_{ch}) \times U}{N_{ch}^{GEN}(N_{pv} = 1, N_{pp} = 1)}$$

The MC multiplicity distribution follows the data exactly after reweighting.

4- New extraction of a reweighted unfolding factor.

New generated and reconstructed corrected distributions are obtained from MC, and a new "reweighted" unfolding factor is obtained as at point 2.

$$U' = \frac{N_{ch}^{GEN}(N_{pv} = 1, N_{pp} = 1) \times W}{N_{ch}^{REC}(N_{pv} = 1) \times PU/C(N_{ch}) \times W}$$

5- Final correction.

A final corrected multiplicity distribution (fig.2) is obtained by applying the new unfolding U' to the distribution corrected with $C(N_{ch})$ of point 1 (the correction for pile-up needs also to be applied).

V SYSTEMATIC UNCERTAINTIES

Eight potential sources of systematics have been outlined:

- A. the amount of undetected pile-up;
- B. the merging of the MB and the high-multiplicity data samples;
- C. the correction for the trigger inefficiency;
- D. the correction for vertex reconstruction inefficiency;
- E. the correction for diffractive background suppression;
- F. the dependence of our correction on the MC generator;
- G. the usage of the dijet-10 MC sample for the correction of the high multiplicity tail of the distribution;
- H. different correction methods in the tail of the distribution.

For each of these we evaluate an uncertainty. All eight are then summed in quadrature (they are largely independent of each other) and the total systematic uncertainty is summed in quadrature to the statistical uncertainty to give a total uncertainty. The total uncertainty is shown in fig.3. The total systematic uncertainty on the average is about 0.2.

A Uncertainty on Pile-Up

Our best estimate of the amount of undetected pile-up is 2.5% of all crossings. The MC sample gives 2.9%. We take the discrepancy (2.9%-2.5%=0.4%) as the systematic uncertainty on the whole range of N_{ch} . This value is added of another 0.1% to take into account the uncertainty on the diffractive cross-section that is used to evaluate the pile-up.

B Merging of the data samples

The data from the MB and the high-multiplicity triggers are merged assuming that their effective trigger cross sections are the same. In the range of $N_{ch} \geq 23$ the normalization of the multiplicity distributions differs of 1.1%. This is taken as a systematic uncertainty in $N_{ch} \geq 23$.

C Trigger Efficiency

There is a systematic uncertainty of about 4.4% on the acceptance of the CLC counters that are used for the minbias trigger. We take this value as the uncertainty on the trigger efficiency correction.

D Vertex Efficiency

The correct number of events depends on the correction for vertex reconstruction inefficiency which was evaluated with MC. This correction, applied to the same MC sample, returns a number of reconstructed vertices that differs of 0.2% from the number of generated ones. These are mostly low-multiplicity events, so the uncertainty affects only the bins of multiplicity zero and one.

E Diffractive Background Suppression

There are two possible uncertainties on the correction for the contamination of diffractive events: the value of the diffractive cross-section with respect to the inelastic-non-diffractive one, and the average number of diffractive particles in the COT region. We let the con-

tribution of diffractive events in MB vary from 5 to 7% and the average multiplicity from 1.0 to 1.4 tracks/event. We take as uncertainty the maximum variation obtained which is about 30% of the correction itself. It ranges from about 12% at $N_{ch}=0$ to negligible values at $N_{ch}>6$.

F Dependence on the MC Generator

The absolute correction applied on N_{ch} may depend on how well the MC generator represents the data, even though the MC sample is reweighted to the data. In order to estimate such dependence, we compute new correction from a sample of Pythia tuned with the “DW” tuning (for a description of the tunings see [17]). Besides the other different parameters, this sample also has CKIN(3)=0, while our tuneA has CKIN(3)=1.5. The tuneDW shows smaller average particle multiplicity than both data and tuneA, but roughly the same p_T spectrum.

The difference produced by different MC configuration on the final corrected distribution is used to evaluate the uncertainty. We plot bin-by-bin the quantity 1 minus the ratio of the distributions corrected with tuneA and tuneDW and take these values as systematic uncertainty. This is probably an overestimate as we already know that the tuneDW distribution does not follow the data as well as tuneA. Similar values are obtained by applying the same method to the inclusive correction distributions. In the region $N_{ch}>40$ tuneDW does not provide enough statistics for a significant evaluation: the systematic is therefore extrapolated from the previous bins.

G Use of the Dijet-10 Sample

In the region above $N_{ch}=35$ the MC generator does not produce enough events to allow a statistically significant correction. For this region we merged the minimum-bias MC with events from a Pythia dijet-10. The topology of the two are very similar but still some difference may produce small variations in the tracking efficiency. We modify the dijet sample by excluding events with a jet of $E_T > 20$ GeV in $|\eta| < 1$ and compare the mean absolute correction ($\langle C(N_{ch}) \rangle$) to that of the full dijet sample and of the MB sample. While the two dijet samples give roughly the same mean correction of $\simeq 92\%$, the MB sample gives

about $\simeq 90\%$ in the available region $N_{ch} \leq 43$. Therefore, in the region $36 \leq N_{ch} \leq 43$, where minbias and dijets events are merged, we evaluate a systematic uncertainty of 1% (half the discrepancy); and in the region $N_{ch} > 43$ of 2% (the full discrepancy). The same comparison is carried on for the all-inclusive correction, which is more dependent on the MC generator. In this case we obtain a difference about twice as large than on the mean absolute correction. To be conservative we then take an uncertainty of 2% in the region $36 \leq N_{ch} \leq 43$ and of 4% in the region $N_{ch} > 43$.

H Correction of the tail

In the region $N_{ch} \geq 50$ our MC statistics is not enough to determine accurately what is the shape of the multiplicity distribution of “true” GEN events at a given REC multiplicity. For this reason we group together the last bins of multiplicity. This operation modifies the distribution of the corresponding GEN events. To evaluate the effect, we compute the correction also by assuming that the correct shape in $N_{ch} \geq 50$ is the same as in the last non-grouped bin (the average obviously changes so that we have the same fitted function just shifted to the right). The effect is to move three events to higher multiplicity that corresponds, on average, to an effect of about 10%. This is taken as an additional uncertainty.

VI RESULTS AND COMPARISON WITH MC

The final corrected multiplicity distribution is shown in fig.2. The average multiplicity is $4.51 \pm 0.02(\text{stat.}) \pm 0.2(\text{syst.})$, while Pythia tuneA has an average of $5.0134 \pm 0.0008(\text{stat.})$.

The statistical uncertainty on each bin of the multiplicity distribution was computed assuming a “multinomial” nature of the distribution. The variance is $np_i(1 - p_i)$ (where p_i is the probability of a given i -th bin of N_{ch}) and its square root was taken as the statistical uncertainty for each bin. The relative statistical uncertainty was summed simply with the relative uncertainties originating from the various corrections.

The distribution obtained shows a complex structure which has never been described in detail. Such structure was already observed at the *SppS* [3]. It may well be caused by the onset of multiple “parton-parton” interactions or of the production of heavier flavors.

For clarity we show the ratio of the corrected distribution to Pythia tuneA in fig.5.

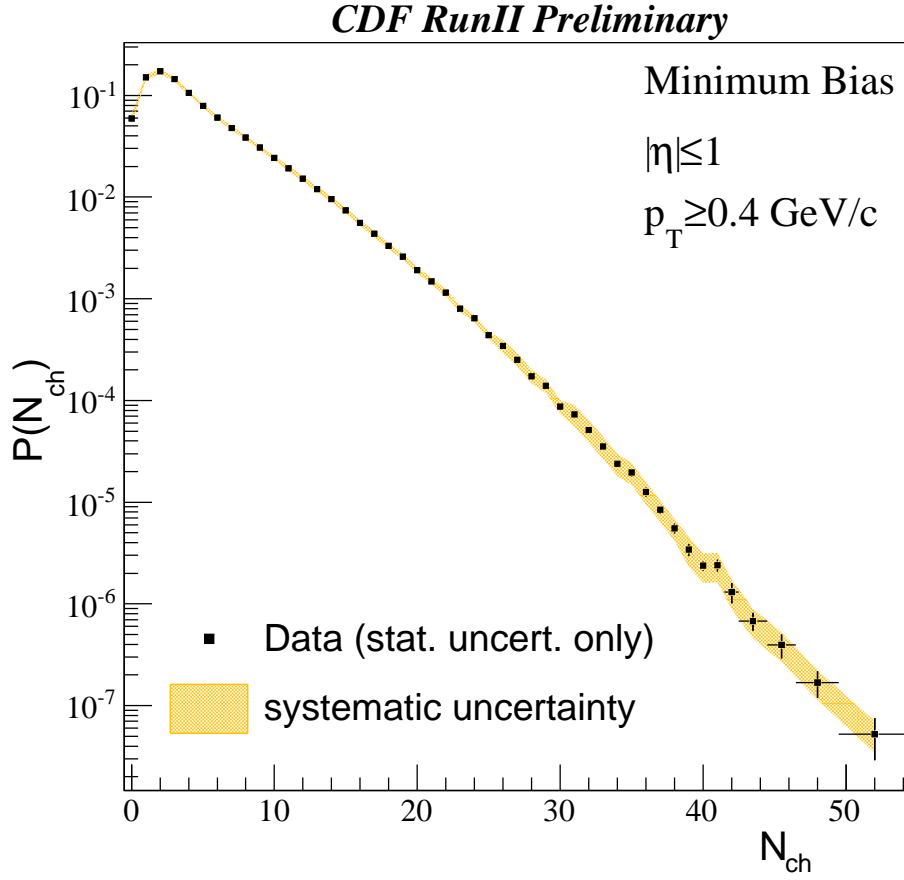


FIG. 2: The corrected multiplicity distribution. Statistical uncertainty is represented as error bars; the band represents the systematic uncertainty.

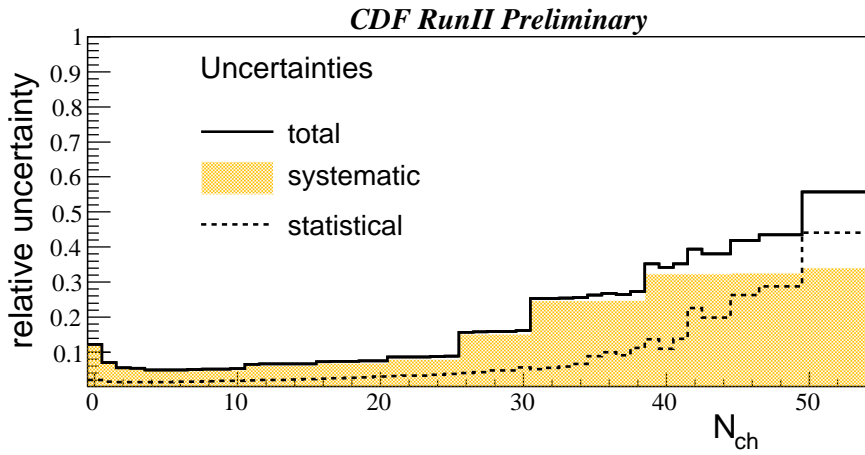


FIG. 3: The total uncertainty as a function of N_{ch} . The statistical and systematic uncertainties are also shown separately.

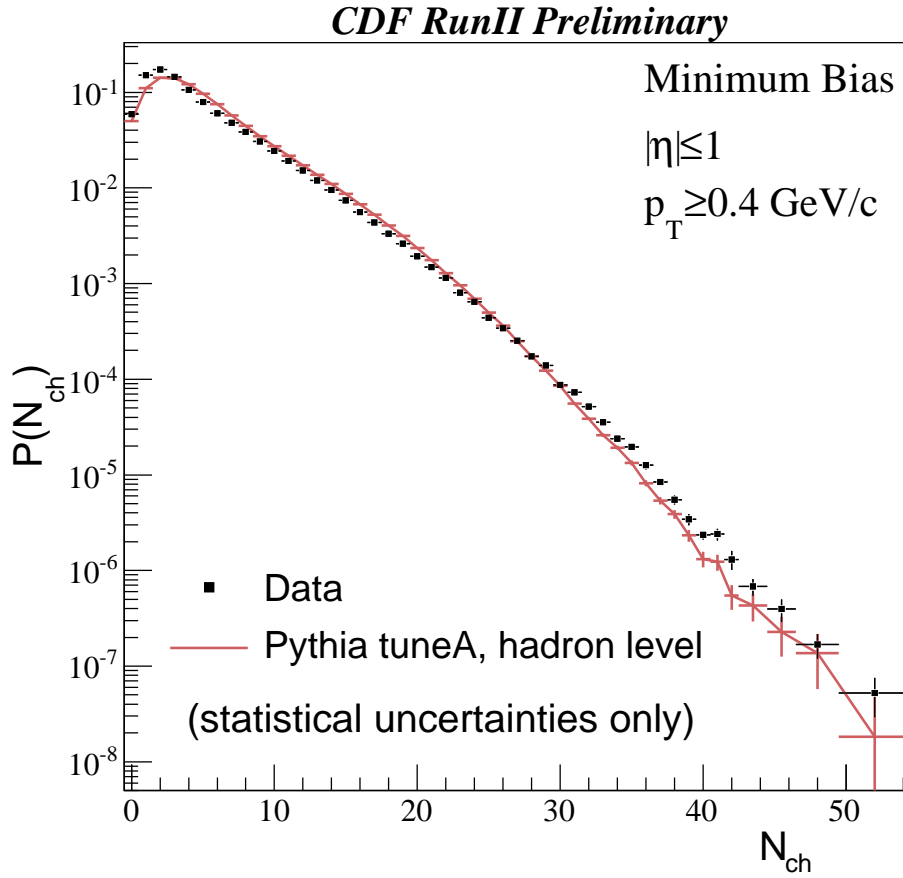


FIG. 4: Comparison of data and PYTHIA tuneA.

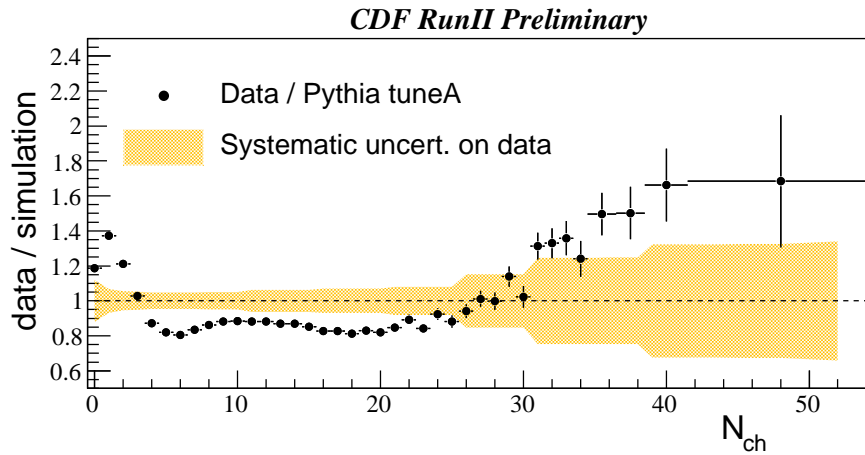


FIG. 5: Ratio of corrected data to Pythia tuneA. A band corresponding to the systematic uncertainty on data is also shown.

ACKNOWLEDGMENTS

We thank the Fermilab staff and the technical staffs of the participating institutions for their vital contributions. This work was supported by the U.S. Department of Energy and National Science Foundation; the Italian Istituto Nazionale di Fisica Nucleare; the Ministry of Education, Culture, Sports, Science and Technology of Japan; the Natural Sciences and Engineering Research Council of Canada; the National Science Council of the Republic of China; the Swiss National Science Foundation; the A.P. Sloan Foundation; the Bundesministerium für Bildung und Forschung, Germany; the World Class University Program, the National Research Foundation of Korea; the Science and Technology Facilities Council and the Royal Society, UK; the Institut National de Physique Nucleaire et Physique des Particules/CNRS; the Russian Foundation for Basic Research; the Ministerio de Ciencia e Innovación, and Programa Consolider-Ingenio 2010, Spain; the Slovak R&D Agency; and the Academy of Finland.

-
- [1] T. Aaltonen *et al.* (CDF Collaboration), *Phys. Rev. D* **79**, 112005 (2009).
 - [2] *Phys.Lett. B* **138**, 304 (1984);
Phys.Rev. D **30**, 528 (1984);
Phys.Lett. B **160**, 193 (1985);
Phys. Lett. C **30**, 391 (1886).
 - [3] *Z.Phys C* **43** 357 (1989).
 - [4] P. Skands and D. Wicke, *Eur. Phys. J. C* **52**, 133 (2007);
P. Skands, Fermilab-Conf-09-113-T; (2009).
 - [5] D. Acosta *et al.* (CDF Collaboration), *Phys. Rev. D* **71**, 032001 (2005);
D. Acosta *et al.* (CDF Collaboration), *Phys. Rev. D* **71**, 052003 (2005);
A. Abulencia *et al.* (CDF Collaboration), *J. Phys. G Nucl. Part. Phys.* **34**, 2457 (2007);
The CDFII Detector Technical Design Report, Fermilab-Pub-96/390-E (2006).
 - [6] D. Acosta *et al.*, *Nucl. Instrum. Methods A* **494**, 57 (2002).
 - [7] D. Acosta *et al.*, *Nucl. Instrum. Methods A* **461**, 540 (2001).
 - [8] D. Acosta *et al.*, *Nucl. Instrum. Methods A* **518**, 605 (2004).

- [9] S. Klimenko, J. Konigsberg and T. M. Liss, Fermilab-Fn-0741 (2003).
- [10] F. Abe *et al.*, (CDF Collaboration), Phys. Rev. D **50**, 5550 (1994);
F. Abe *et al.*, (CDF Collaboration), Phys. Rev. D **50**, 5535 (1994);.
- [11] T. Sjöstrand *et al.*, High-Energy-Physics Event Generation with PYTHIA 6.1, Comput. Phys. Commun. **135** 238, (2001);
T. Sjöstrand, Phys. Lett. B **157**, 321 (1985);
T. Sjöstrand and M. van Zijl, Phys. Rev. D **36**, 2019 (1987).
- [12] R. Field, AIP Conf. Proc. **828**, 163 (2006);
R. Field, Acta Physica Polonica B **36**, 167 (2005);
D. Acosta *et al.* (CDF Collaboration), Phys. Rev. D **70**, 072002 (2004).
- [13] T. Sjöstrand and P. Skands, Eur. Phys. J., C **39**, 129 (2005).
- [14] H. L. Lai *et al.* (CTEQ Collaboration), Eur. Phys. J. C **12**, 375 (2000).
- [15] B. Andersson, Camb. Monogr. Part. Phys. Nucl. Phys. Cosmol. **7**, 1 (1997).
- [16] \hat{p}_{T^0} is defined as the transverse momentum of the 2-to-2 scattering in the rest frame of the hard interaction.
- [17] R. Field, Pub. Proc. 33rd Int. Conf. on High Energy Physics, Moscow, Russia (2006);
R. Field, Pub. Proc. TeV4LHC Workshop, Fermilab, Batavia IL, USA (2005).